NPS-53Zh51Wu75091

NAVAL POSTGRADUATE SCHOOL

Monterey, California

THE COMPUTATIONAL STABILITY PROPERTIES OF THE SHUMAN PRESSURE GRADIENT AVERAGING TECHNIQUE

Arthur L. Schoenstadt and R. T. Williams

September 1975

Prepared for:
Chief of Naval Research, Arlington, Virginia 22217
Fleet Numerical Weather Central, Monterey, California 93940
...mental Prediction Research Facility, Monterey,
...nia 93940

NAVAL POSTGRADUATE SCHOOL
Monterey, California

Rear Admiral Isham Linder
Superintendent

Jack R. Borsting
Provost

The work reported herein was supported in part by the Foundation Research Program of the Naval Postgraduate School with funds provided by the Chief of Naval Research, and in part by Fleet Numerical Weather Central and the Environmental Prediction Research Facility.

This report was prepared by:

UNCLASSIFIED

SECURITY CLASSIFICATION OF THIS PAGE *(When Data Entered)*

REPORT DOCUMENTATION PAGE		READ INSTRUCTIONS BEFORE COMPLETING FORM
1. REPORT NUMBER NPS-53Zh51Wu75091	2. GOVT ACCESSION NO.	3. RECIPIENT'S CATALOG NUMBER
4. TITLE *(and Subtitle)* THE COMPUTATIONAL STABILITY PROPERTIES OF THE SHUMAN PRESSURE GRADIENT AVERAGING TECHNIQUE		5. TYPE OF REPORT & PERIOD COVERED Final 6. PERFORMING ORG. REPORT NUMBER
7. AUTHOR*(s)* Arthur L. Schoenstadt R. T. Williams		8. CONTRACT OR GRANT NUMBER*(s)*
9. PERFORMING ORGANIZATION NAME AND ADDRESS Naval Postgraduate School Monterey, California 93940		10. PROGRAM ELEMENT, PROJECT, TASK AREA & WORK UNIT NUMBERS 61152N; RR000-01-10 N0001475WR50001
11. CONTROLLING OFFICE NAME AND ADDRESS Chief of Naval Research, Arlington, VA 22217 Fleet Numerical Weather Central, Monterey, CA 93940		12. REPORT DATE September 1975 13. NUMBER OF PAGES 29
14. MONITORING AGENCY NAME & ADDRESS*(if different from Controlling Office)*		15. SECURITY CLASS. *(of this report)* UNCLASSIFIED 15a. DECLASSIFICATION/DOWNGRADING SCHEDULE

16. DISTRIBUTION STATEMENT *(of this Report)*

Approved for public release; distribution unlimited.

17. DISTRIBUTION STATEMENT *(of the abstract entered in Block 20, if different from Report)*

18. SUPPLEMENTARY NOTES

19. KEY WORDS *(Continue on reverse side if necessary and identify by block number)*

Computational Stability
Finite Difference Methods
Finite Difference Solutions
Numerical Weather Prediction
Numerical Methods
Primitive Equations of Meteorology

20. ABSTRACT *(Continue on reverse side if necessary and identify by block number)*

The stability properties of the Shuman pressure gradient averaging technique are investigated with the linearized shallow water equations. In the simplest case an analytic expression is obtained for the stability region, and the maximum time step is shown to be twice the value for the leapfrog scheme. When a mean flow is added to the equations, it is shown the maximum time step must be reduced. The time averaging suggested by Robert is examined, and again leads to a shorter time step. In each case,

DD FORM 1 JAN 73 1473 EDITION OF 1 NOV 65 IS OBSOLETE
S/N 0102-014-6601 |

UNCLASSIFIED

SECURITY CLASSIFICATION OF THIS PAGE *(When Data Entered)*

11. Environmental Prediction Research Facility
Monterey, CA 93940

20. however, the use of the Shuman averaging allows a significantly longer time step than the conventional leapfrog scheme.

SUMMARY

The centered difference leapfrog technique, commonly used in the numerical solution of the primitive equations of meteorology, computes the gradient of the geopotential at the n^{th} time step by:

$$\frac{\partial \phi}{\partial x}(t_n, x_j) = \frac{1}{2\Delta x}\{\phi^n_{j+1} - \phi^n_{j-1}\},$$

where:

$$\phi^n_j = \phi(t_n, x_j) .$$

The Shuman technique replaces this term by a weighted average of the centered differences on the $(n-1)^{st}$, n^{th}, and $(n+1)^{st}$ time steps. This should allow the use of a longer time step than that predicted by the CFL condition before the onset of computational instability. This paper considers the computational stability regions obtainable by this technique in the cases of: (1) the linearized barotropic model with no Coriolis force and no mean flow, (2) the linearized barotropic model with no Coriolis force, but including a mean flow, (3) the linearized barotropic model with no Coriolis force and no mean flow, but incorporating the time filtering technique designed by Robert, and, (4) the linearized barotropic model with no Coriolis force, but including a mean flow and time filtering. In each of these cases, the Shuman technique is demonstrated to yield an increased time step and the maximum size of the time steps is shown. The presence of a mean flow or filtering yields maximum time steps lower than those of basic solution (case (1)), but still significantly higher than the unaveraged method.

TABLE OF CONTENTS

LIST OF FIGURES

1. Introduction

Shuman [6] has proposed a modification to the leapfrog scheme for the primitive equations which are used in numerical weather prediction. The scheme which uses a weighted average of the pressure gradient at the past, present and future times, allows a longer time step than the one given by the CFL condition. Brown and Campana [2] have carried out the linear analysis of this modification for the three cases: (1) the barotropic model, (2) a two-layer model whose pressure is the vertical coordinate, and (3) a two-layer model with the Phillips [4] sigma coordinate system. In this paper we will treat only the linearized barotropic model. We will present an analytic solution for the computational stability curve for the simplest case. A mean flow will be added to the equations and the stability curve will be obtained numerically and also with an approximate analytic procedure. Finally the time filter designed by Robert [5] will be applied to all variables and the resulting stability curve will be presented. It will be seen that both the presence of a mean flow and the time filtering reduce the time step, but that the use of the Shuman technique is still advantageous.

2. Basic solution

The linearized equations for the barotropic model with no Coriolis force and no mean flow are:

$$\frac{\partial u}{\partial t} = - \frac{\partial \phi}{\partial x} , \tag{1}$$

$$\frac{\partial \phi}{\partial t} = -\Phi \frac{\partial u}{\partial x} . \tag{2}$$

Here u is the velocity component in the x-direction and ϕ/g is the departure of the free surface height from its mean value Φ/g . These

equations describe shallow water waves which move with speed $\sqrt{\Phi}$.

The finite difference approximations to equations (1) and (2) with the Shuman pressure gradient averaging included are:

$$\frac{u_j^{n+1}-u_j^{n-1}}{2\Delta t} + \frac{1}{2\Delta x}\left[\phi_{j+1}^n-\phi_{j-1}^n+\alpha[\phi_{j+1}^{n+1}-\phi_{j-1}^{n+1}+\phi_{j+1}^{n-1}-\phi_{j-1}^{n-1}-2(\phi_{j+1}^n-\phi_{j-1}^n)]\right] = 0 \ , \quad (3)$$

$$\frac{\phi_j^{n+1}-\phi_j^{n-1}}{2\Delta t} + \Phi\left(\frac{u_{j+1}^n-u_{j-1}^n}{2\Delta x}\right) = 0 \ , \quad (4)$$

where the discretization uses $x = j\Delta x$ and $t = n\Delta t$. The usual leapfrog differencing is obtained by setting $\alpha = 0$. This scheme is explicit since ϕ^{n+1} may be obtained from (4) before it is needed in (3).

In order to obtain the computational stability properties of this scheme we substitute the following expressions

$$\begin{aligned} u_j^n &= A\,\omega^n\, e^{ik\Delta xj} \\ \phi_j^n &= B\,\omega^n\, e^{ik\Delta xj} \end{aligned} \ , \quad (5)$$

into (3) and (4). After the constants A and B have been eliminated we obtain the following quartic equation for ω:

$$\omega^4 + 4S\alpha\,\omega^3 - 2[1-2S(1-2\alpha)]\,\omega^2 + 4S\alpha\,\omega + 1 = 0 \ , \quad (6)$$

where

$$S \equiv \left(\frac{\Delta t}{\Delta x}\right)^2 \Phi \sin^2 k\Delta x \ . \quad (7)$$

Since S and α are real, the roots of (6) are either real or in complex conjugate pairs. Due to the symmetry in the differencing we expect that $|\omega| = 1$ for some range of the parameters. As a result the polynomial factors to

$$(\omega^2 + 2a_1\omega + 1)\,(\omega^2 + 2a_2\omega + 1) = 0 \ . \quad (8)$$

If we expand (8) and compare with (6) we find that a_1 and a_2 must satisfy the following equation:

$$a_i^2 - 2S\alpha\, a_i + S(1-2\alpha) - 1 = 0 , \quad i = 1,2 . \tag{9}$$

The solutions to this equation are

$$a_i = S\alpha \pm \sqrt{(S\alpha+1)^2 - S} . \tag{10}$$

It can be seen from (8) that only when the a_i's are real and of magnitude less than or equal to unity will all the roots of (8) have $|\omega| = 1$. The value of a_i will be real when the quantity under the radical is non-negative; therefore, this condition can be written

$$(S\alpha + 1)^2 - S \geq 0 . \tag{11}$$

If we choose the equality we will obtain the following stability relation:

$$S = \frac{1 - 2\alpha - \sqrt{1 - 4\alpha}}{2\alpha^2} , \tag{12}$$

where the minus sign in front of the radical was chosen to make the expression reasonable in the limit as $\alpha \to 0$. The condition that the a_i's have magnitude not greater than 1 leads to the condition

$$\alpha \leq \frac{1}{4} . \tag{13}$$

This is consistent with (12) which becomes complex for $\alpha > \frac{1}{4}$.

The combination of conditions (12) and (13) is given in Fig. 1 as the curve labeled $\sigma = 0$. Brown and Campana [2] determined a curve with approximately this shape by numerically solving for the roots of (6); however, they did not present its analytic form (12). The maximum value of S which is $S = 4$, occurs at $\alpha = \frac{1}{4}$. For the usual leapfrog

differencing ($\alpha = 0$) the maximum value of S which allows computationally stable solutions is $S = 1$. Since S is proportional to Δt^2 (see Eq.(7)) it follows that the use of the Shuman pressure gradient averaging in this linear system allows a doubling of the time step as compared with the standard leapfrog scheme. However it may be difficult to achieve this factor of 2 in practice when other effects are included since the width of the stable region goes to zero as S approaches 4 . In fact a value of α which is slightly less than $\frac{1}{4}$ would probably be preferable.

3. Solutions with mean flow

In this section we add the effects of a constant mean flow to the stability analysis. The linearized equations are:

$$\frac{\partial u}{\partial t} + U \frac{\partial u}{\partial x} = - \frac{\partial \phi}{\partial x} , \tag{14}$$

$$\frac{\partial \phi}{\partial t} + U \frac{\partial \phi}{\partial x} = - \Phi \frac{\partial u}{\partial x} . \tag{15}$$

Normally the addition of the mean flow terms does not have a great effect on the computational stability criteria since the phase speed of the external gravity waves, $\Phi^{1/2}$, is generally much greater than the speed of the mean wind, U .

When Eqs. (14) and (15) are put in finite difference form with the use of the approximations in (3) and (4), the mean advection terms are evaluated with centered finite differences, and the relations (5) are substituted into the finite difference forms of (14) and (15), we obtain the following equation for ω :

$$\omega^4 + 4(S\alpha + i\sigma)\,\omega^3 + 2[2S(1-2\alpha) - (1+2\sigma^2)]\,\omega^2 + 4(S\alpha - i\sigma)\,\omega + 1 = 0 , \tag{16}$$

where

$$\sigma = \frac{U\Delta t}{\Delta x} \sin k\Delta x . \tag{17}$$

Note that dividing (16) by ω^4 and taking the complex conjugate of the equation, yields an equation in $1/\omega^*$ with the same coefficients as (16). Thus, it follows that ω is a root of (16) if and only if $(\omega^*)^{-1}$ is also a root, and therefore the roots must be distributed in exactly one of the following ways:

Case I: Four roots (including multiple roots) on the unit circle

$$(e^{i\phi_1},\ e^{i\phi_2},\ e^{i\phi_3},\ e^{i\phi_4};\ \phi_1 + \phi_2 + \phi_3 = -\phi_4) .$$

Case II: Two roots on the unit circle, two roots off the unit circle

$$(e^{i\phi_2},\ e^{i\phi_3},\ \rho e^{i\phi_1},\ \frac{1}{\rho} e^{i\phi_1};\ 2\phi_1 + \phi_2 = -\phi_3) .$$

Case III: Four roots off the unit circle

$$(\rho e^{i\phi},\ \frac{1}{\rho} e^{i\phi},\ \zeta e^{-i\phi},\ \frac{1}{\zeta} e^{-i\phi},\ \rho,\zeta \neq 1)$$

In each case the fact that the product of the roots is equal to the last term in (16) was used.

The analysis of Cases I - III indicates that (16) has at least one factorization of the form

$$(\omega^2 + 2ae^{i\theta/2}\ \omega + e^{i\theta})\ (\omega^2 + 2be^{-i\theta/2}\ \omega + e^{-i\theta}) = 0 , \qquad (18)$$

for some angle θ, and a and b real. Furthermore it is easily shown, by analyzing the possible combinations, that in either of the unstable cases (Cases II or III), the factorization (18) must be unique and either a or b (or both) greater than unity in magnitude, whereas the stable case will generally have three distinct representations with both a and b less than or equal to unity in magnitude. The only exception will be when stable, but degenerate (multiple) roots occur.

If we expand (18) and compare with (16) we can obtain the following equations:

$$a = S\alpha \sec \theta/2 + \sigma \csc \theta/2 , \tag{19}$$

$$b = S\alpha \sec \theta/2 - \sigma \csc \theta/2 , \tag{20}$$

$$S^2\alpha^2 \sec^2 \theta/2 - S + S\alpha + \cos^2 \theta/2 - \sigma^2 \cot^2 \theta/2 = 0 . \tag{21}$$

When we write $u = \cos^2 \theta/2$ and use trigonometric identities we can obtain the following polynomial in u :

$$P_\sigma(u) \equiv (u-1)\ (u^2 + S(2\alpha-1)\ u + S^2\alpha^2) + \sigma^2 u^2 = 0 , \tag{22}$$

where one different factorization of the form (18) arises from each distinct solution of (22) in $0 \leq u \leq 1$. Thus by our above comments a sufficient condition for stability is that (22) have more than one solution in [0,1]. The appearance of (22) as a cubic should be expected, since as noted above in the generalized case of stability, we expect three distinct factorizations. When only one solution of (22) occurs in [0,1], then there must be instability unless (16) has a triple root. It can be shown that there is at most one value of σ for which (16) has a triple root.

With this characterization consider the qualitative behavior of $P_\sigma(u)$. Note for all $u > 0$, $\sigma > 0$ that $P_\sigma(u)$ will lie above the curve

$$P_o(u) = (u-1)\ (u^2 + S(2\alpha-1)\ u + S^2\alpha^2) , \tag{23}$$

where it is easily seen that

$$P_o(0) = P_\sigma(0) = - S^2\alpha^2 , \tag{24}$$

$$P_o(1) = 0 , \tag{25}$$

$$P_o'(1) = (S\alpha + 1)^2 - S . \tag{26}$$

Also note that for fixed u, $P'_\sigma(u)$ is a strictly increasing function of σ. These observations now allow us to visualize fairly easily how an instability develops. Consider Fig. 2, which shows a typical situation when $P_o(u)$ has three distinct roots in $0 \leq u \leq 1$, i.e. $\sigma = 0$ yields a stable procedure. Then observe that as σ increases the curve moves upward, causing the value of the smaller root to decrease, and the two larger roots to move closer together. Eventually, for some value σ_{max}, the larger two roots degenerate to a single double root with $P_{\sigma_{max}}(u)$ tangent to the axis there. Finally for $\sigma > \sigma_{max}$, the curve detaches from the axis, leaving only the single smaller root, and hence instability must occur.

Intriguingly, this construction also allows us to visualize a situation when $\sigma > 0$ will yield a stable procedure even though $\sigma = 0$ does not. This is shown in Fig. 3, where as σ increases the curve first attaches itself producing a double lower root, which then moves apart, until eventually a double upper root appears, followed by instability. Numerical solution of (16) verifies this in fact occurs, as evidenced by the curves for $\alpha > \frac{1}{4}$ in Fig. 1.

Now consider the situation when $P'_o(1) > 0$ and $0 \leq \alpha \leq \frac{1}{4}$. The roots of $P_o(u) = 0$ are

$$u_o = 1 , \tag{27}$$

$$u_1 = \frac{S}{2}\left[(1-2\alpha) - \sqrt{1-4\alpha}\right] , \tag{28}$$

$$u_2 = \frac{S}{2}\left[(1-2\alpha) + \sqrt{1-4\alpha}\right] . \tag{29}$$

Since $(1-4\alpha) \leq (1-2\alpha)^2$ it follows that $P_o(u)$ has a shape as indicated in Fig. 2. The maximum stable value of σ (hereafter called σ_{max}) occurs when the larger root of $P'_\sigma(u) = 0$ is also a double root of $P_o(u)$.

Since $P_\sigma(u)$ is a cubic the conditions can be worked our formally; however, the resulting conditions are too cumbersome to provide computational or analytic insights. Therefore we shall present some simpler necessary conditions and approximate expressions.

First, observe that if $P_o'(u) \leq 0$, $P_o(u)$ has exactly one root in $0 < u < 1$, hence $P_\sigma(u)$ must have exactly one root in $0 \leq u \leq 1$. Thus $P_o'(u) > 0$ is a necessary condition for stability when $\sigma > 0$. (Observe the condition that (26) be non-negative is identical to (11).)

A rather accurate approximation to σ_{max} for this situation can be obtained by noting that the onset of instability must correspond to $a = 1$, since $a > 1$ yields, from (18), a solution with $|\omega| > 1$. Thus from (19) σ_{max} satisfies

$$S\alpha \sec \theta/2 + \sigma_{max} \csc \theta/2 = 1 ,$$

or

$$\frac{S\alpha}{\sqrt{u_L}} + \frac{\sigma_{max}}{\sqrt{1-u_L}} = 1 , \tag{30}$$

where u_L denotes the smallest root of $P_{\sigma_{max}}(u)$. This is necessary since both a and b must be continuously dependent on σ.

The u_L in (30) is not known exactly, but the examination of Fig. 2 indicates that

$$u_L \sim u_1 , \tag{31}$$

where u_1 is the lower root of $P_o(u)$. Thus to a first approximation, stability will occur for

$$0 \leq \sigma_{max} \cong \sqrt{1 - u_1} \left\{ 1 - \frac{S\alpha}{\sqrt{u_1}} \right\} , \quad 0 < \alpha < \frac{1}{4} , \tag{32}$$

where u_1 is given by (28). It will be seen that this equation gives an excellent approximation to the values obtained numerically. Unfortunately, a similar approximation for $\frac{1}{4} < \alpha$ has not yet been found.

The roots of (16) were computed numerically and the resulting stability curves are given in Fig. 1 for selected values of σ. All the curves in Fig. 1 have similar shapes with the lowest curves corresponding to the highest values of σ. The following stability condition for $\alpha = 0$ is easily obtained:

$$S^{1/2} + |\sigma| \leq 1 \ . \tag{33}$$

For $\sigma = 0.1$ the increase in Δt over the value for $\alpha = 0$ (see equation (17)) is about 80 percent. A typical value of σ for operational numerical prediction models would be between 0.1 and 0.2. Fig. 1 also shows that stability can occur for the larger values of σ in the region $\alpha > \frac{1}{4}$. However these values of α should not be used because there will always be a value of $k\Delta x$ in (17) which will give an arbitrarily small value of σ and therefore instability.

Tables 1 and 2 compare values on the numerical stability curve from Fig. 1 with values computed from (30). The agreement is quite good with the largest difference occurring for α near $\frac{1}{4}$ and for larger values of σ.

4. Solutions with time filter

Time filtering has been used in numerical weather prediction models to damp both physical and numerical noise (Robert [5], Haltiner and McCollough [3]). Consider the following centered time filter:

$$\bar{F}(t) = F(t) + \gamma[F(t + \Delta t) + \bar{F}(t - \Delta t) - 2F(t)] \ . \tag{34}$$

This form is convenient for operational prediction because it uses the previous averaged value which saves machine storage. When this filter is used in linear equations which have solutions proportional to ω^n, equation (34) takes the form

$$\bar{F}(t) = (F(t) + \gamma[F(t + \Delta t) - 2F(t)]/(1 - \gamma\omega^{-1}) \quad . \tag{35}$$

Here we have used the relation $\bar{F}(t - \Delta t) = \omega^{-1} \bar{F}(t)$.

This time filter is introduced into the finite difference equations (3) and (4) by replacing u_j^{n-1} and ϕ_j^{n-1} with the filtered values obtained from (35). When the relations (5) are introduced into the time averaged difference equations we obtain the following equation:

$$\omega^4 + 4[S\alpha-\gamma]\,\omega^3 + \left[4\left(\gamma(1+\gamma) + S[1-2\alpha(1+\gamma)]\right)-2\right]\omega^2$$
$$+ 4[S(\alpha(1+2\gamma)-2\gamma) + \gamma(1-2\gamma)]\,\omega + 4S\gamma(\gamma-\alpha) + (1-2\gamma)^2 = 0 \quad . \tag{36}$$

If we consider the special case of no pressure gradient averaging ($\alpha = 0$), the equation reduces to

$$[\omega^2 - 2\gamma\omega - (1-2\gamma)]^2 = -4S(\omega-\gamma)^2 \quad . \tag{37}$$

Take the square root of both sides of this equation and solve for ω which yields

$$\omega = \gamma \pm iS^{1/2} \pm \sqrt{(\gamma-1)^2 - S} \quad . \tag{38}$$

This result was obtained by Asselin [1] who has discussed the solutions in detail. When S is sufficiently small the solutions will be damped. The critical value of S which is always less than 1, decreases as γ increases. However, in the damping region, the damping rate increases with increasing γ .

In the general case the roots to (36) must be found numerically. Fig. 4 contains the curves which separate the unstable solutions from the stable solutions for selected values of γ. The left hand limits of the curves show the reduction in the critical S as a function of γ for $\alpha = 0$. The curve for $\gamma = .05$ closely approximates the curve for $\sigma = 0$ in Fig. 1. As γ increases the maximum stable value decreases and shifts to the right. In fact sizable stable regions exist for $\alpha > \frac{1}{4}$ depending on γ. For $\gamma = 0$ there are no stable solutions for $\alpha > \frac{1}{4}$.

We now consider the effect of the time averaging on the solutions when the mean flow is included. When the time averaging effects are added to equation (16) we obtain:

$$\omega^4 + 4[S\alpha - \gamma + i\sigma]\omega^3 + [4(\gamma(\gamma+1) - \sigma^2 + S(1-2\alpha(\gamma+1))) - 2 - 12\sigma\gamma i]\,\omega^2$$
$$+ 4[S(\alpha(1+2\gamma)-2\gamma) + \gamma(1-2\gamma+2\gamma^2) + i\sigma(2\gamma(\gamma+1)-1]\,\omega$$
$$+ 4S\gamma(\gamma(1-\sigma^2)-\alpha) + (1-2\gamma)^2 + i4\sigma\gamma(1-2\gamma) = 0 . \qquad (39)$$

Fig. 5 contains the stability curves which were obtained by numerical solution of (39) for the value $\sigma = 0.1$. The curves which are for $\gamma = 0.1, 0.2, 0.3$ show smaller values of maximum values of S than are seen in Fig. 3. However the starting points ($\alpha = 0$) are also smaller. In general the peaks are located at about the same values of α and the peaks are broader. Both Figs. 4 and 5 show a large improvement in maximum S over the value with no pressure gradient averaging ($\alpha = 0$).

5. Conclusions

The stability properties of the Shuman [6] pressure gradient averaging technique have been investigated in this paper with the linearized shallow water equations. The analytic solution obtained in Section 2 shows that the time step can be doubled for $\alpha = \frac{1}{4}$. However, the width of the stable

region becomes very narrow as $\alpha = \frac{1}{4}$ is approached so that the best value of σ would be slightly less than $\frac{1}{4}$. When a mean flow is included the time step must be reduced. However for reasonable values of the mean flow (σ = 0.1 to 0.2) the time step can still be increased by 70 to 80 percent. The time averaging of all variables which was suggested by Robert [5] has been used to damp unwanted high frequency components in numerical forecasts. The use of the time filtering, however, requires a smaller time step and therefore more computation time. When the time filtering is used in conjunction with the pressure gradient averaging, the time step can be significantly increased although for the larger values of γ the time step may not be much larger than with no time or pressure gradient averaging. When the time averaging is used the optimum value of α is critically dependent on γ. The addition of the mean flow decreases the time step, but does not appreciably affect the optimal α.

The Shuman [6] pressure gradient averaging technique has been used operationally at the National Meteorological Center and it is now undergoing tests at the Fleet Numerical Weather Central. This technique should be useful in other fluid dynamical applications provided that the velocities are appreciably less than the fastest gravity waves.

Acknowledgments: The authors wish to thank Prof. G. J. Haltiner for reading the manuscript and for making several useful comments on it. The manuscript was carefully typed by Ms. M. Marks and the figures were drafted by Mr. P. Adler. A. L. Schoenstadt was supported by the Foundation Research Program of the Naval Postgraduate School which is funded by the Chief of Naval Research. R. T. Williams was supported by the Fleet Numerical Weather Central and the Environmental Prediction Research Facility, both in Monterey, Calif. The numerical computations were performed by the W. R. Church Computer Center.

REFERENCES

1. R. A. ASSELIN, Mon. Wea. Rev., 100 (1972), 487.

2. J. BROWN and K. CAMPANA, "A New Explicit Differencing System for Primitive Equations." National Meteorological Center Office Note (1974).

3. G. J. HALTINER and J. M. McCOLLOUGH, J. Appl. Meteor., 14 (1975), 281.

4. N. A. PHILLIPS, J. Meteor., 14 (1957), 184.

5. A. J. ROBERT, J. Meteor. Soc. Jap., 44 (1966), 237.

6. F. G. SHUMAN, "Resuscitation of an Integration Procedure." National Meteorological Center Office 54 (1971).

TABLES

α	0	0.1	0.2	0.225	0.25
S_{an}	0.78	1.00	1.50	1.75	2.62
S_{num}	0.80	1.02	1.55	1.80	2.50

Table 1. Comparison of the values of S on the stability curve from Fig. 1 (S_{num}) with the values of S computed from Eq. (30) (S_{an}) for $\sigma = 0.1$.

α	0	0.1	0.2	0.225	0.25
S_{an}	0.33	0.43	0.61	0.71	1.04
S_{num}	0.35	0.46	0.62	0.74	0.88

Table 2. Same as Table 1 except for $\sigma = 0.4$.

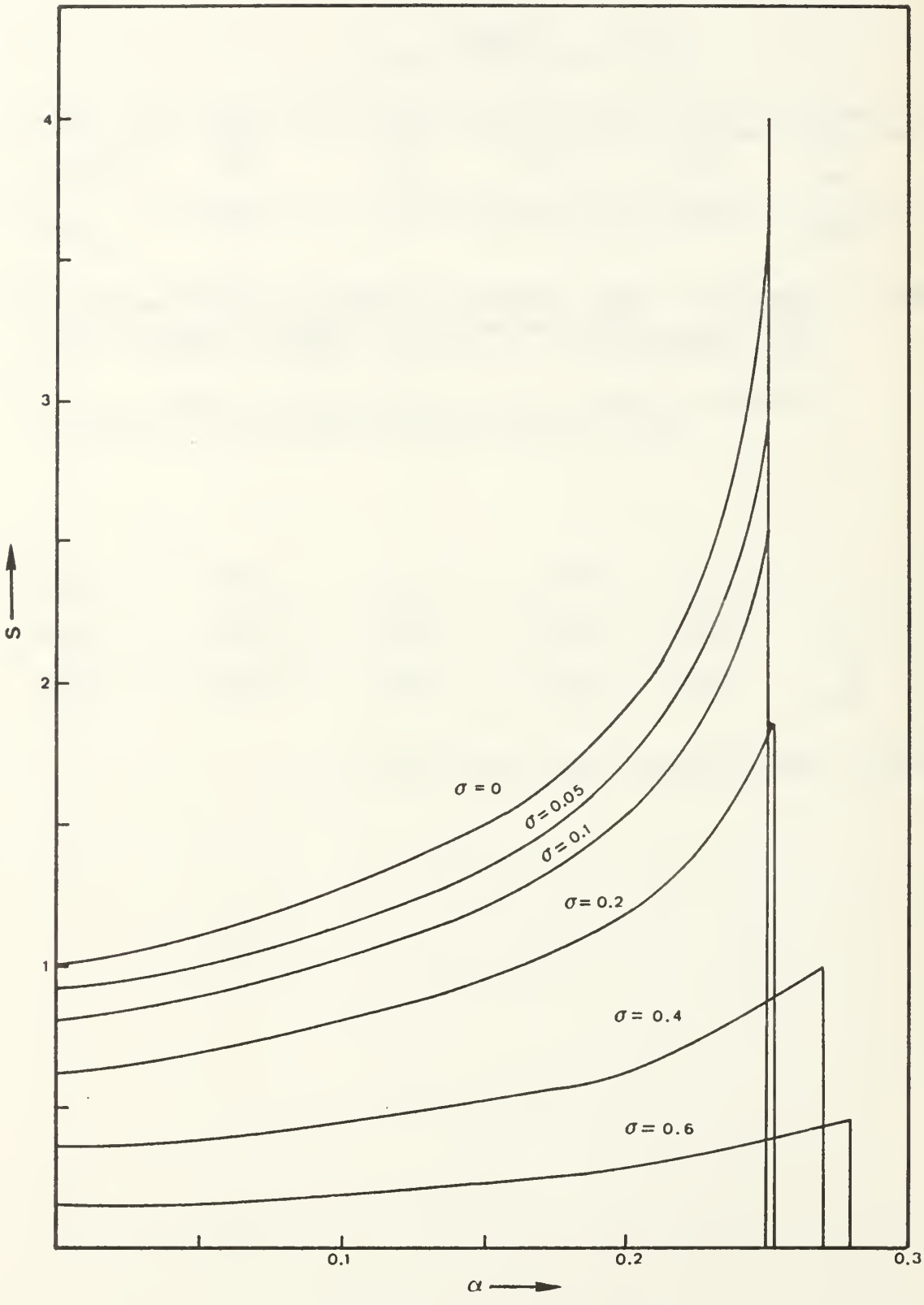
4
3
2
1
S
σ = 0
σ = 0.05
σ = 0.1
σ = 0.2
σ = 0.4
σ = 0.6
0.1
0.2
0.3
α

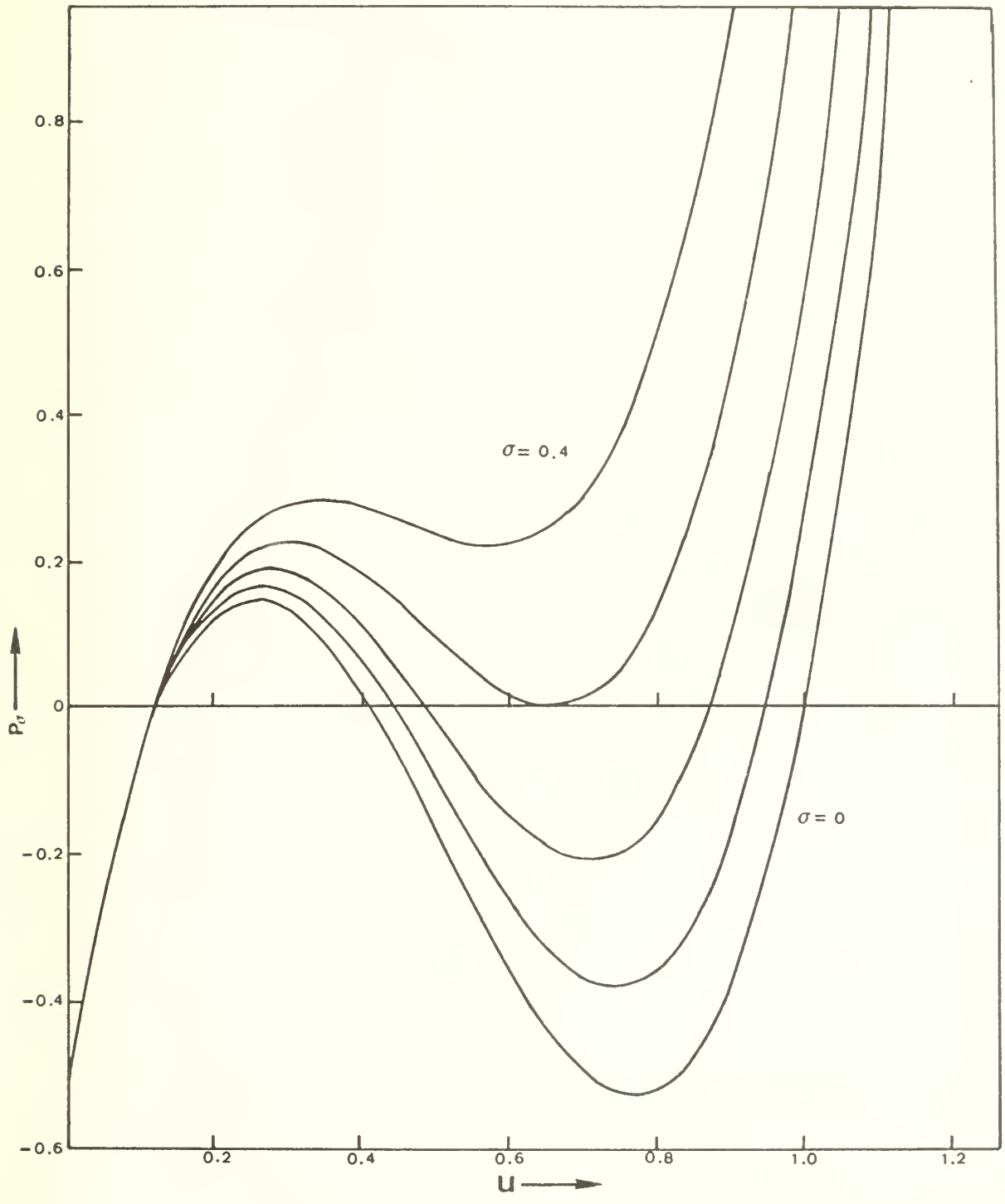
0.8
0.6
0.4
0.2
0
-0.2
-0.4
-0.6
P_v
$\sigma = 0.4$
$\sigma = 0$
0.2
0.4
0.6
0.8
1.0
1.2
u

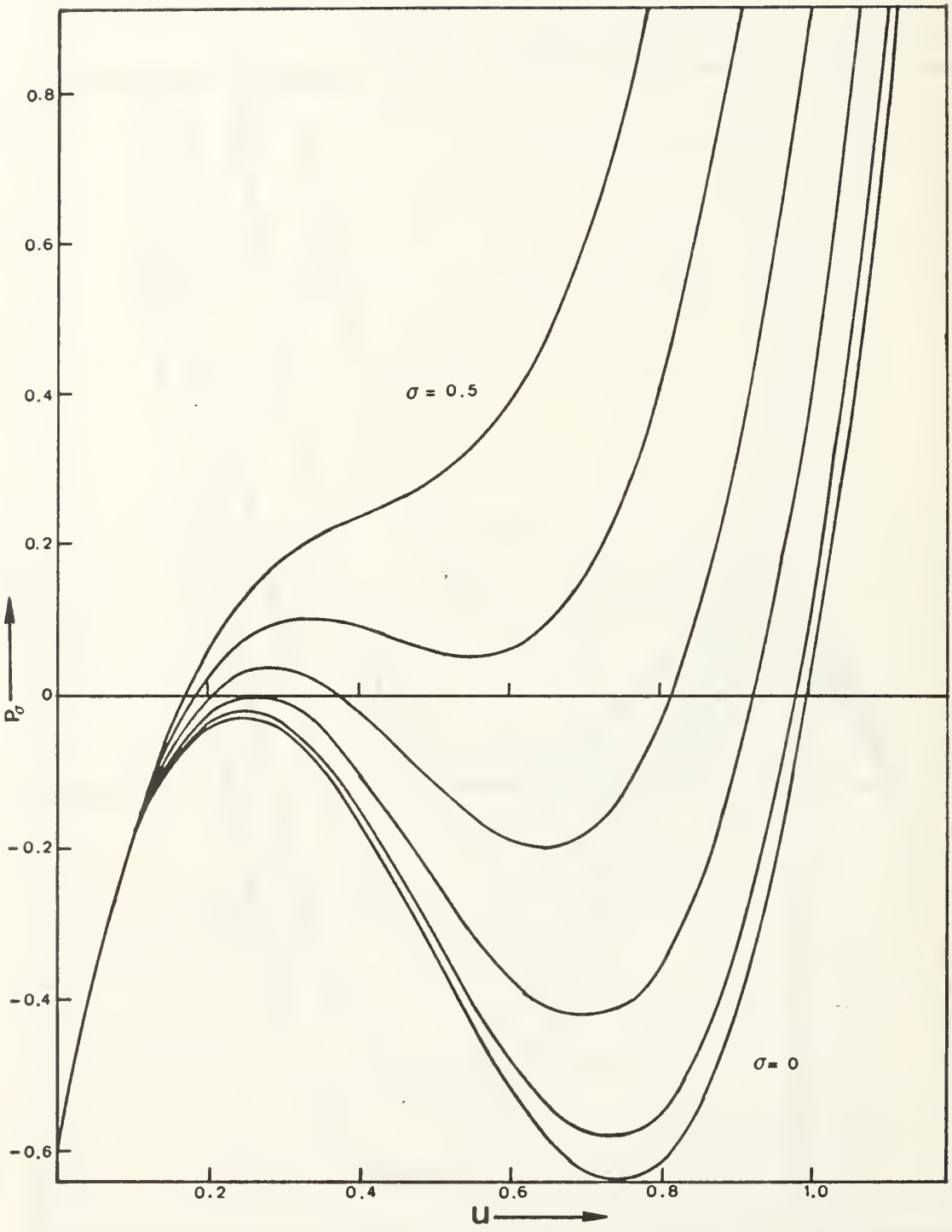
0.8
0.6
0.4
0.2
0
-0.2
-0.4
-0.6
P_σ
$\sigma = 0.5$
$\sigma = 0$
0.2
0.4
0.6
0.8
1.0
u

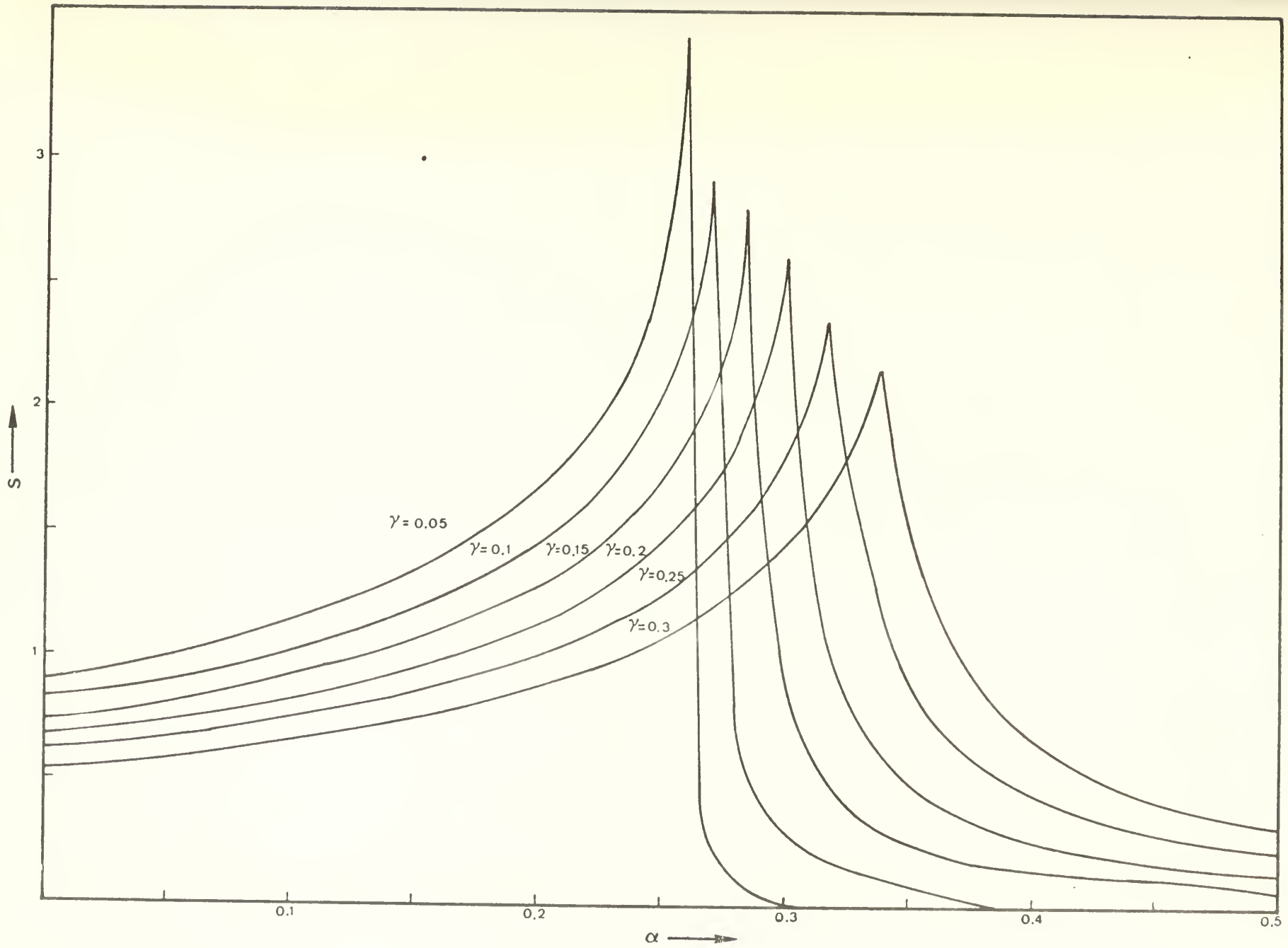
3
2
1
S
γ = 0.05
γ= 0.1
γ=0.15
γ=0.2
γ=0.25
γ=0.3
0.1
0.2
0.3
0.4
0.5
α

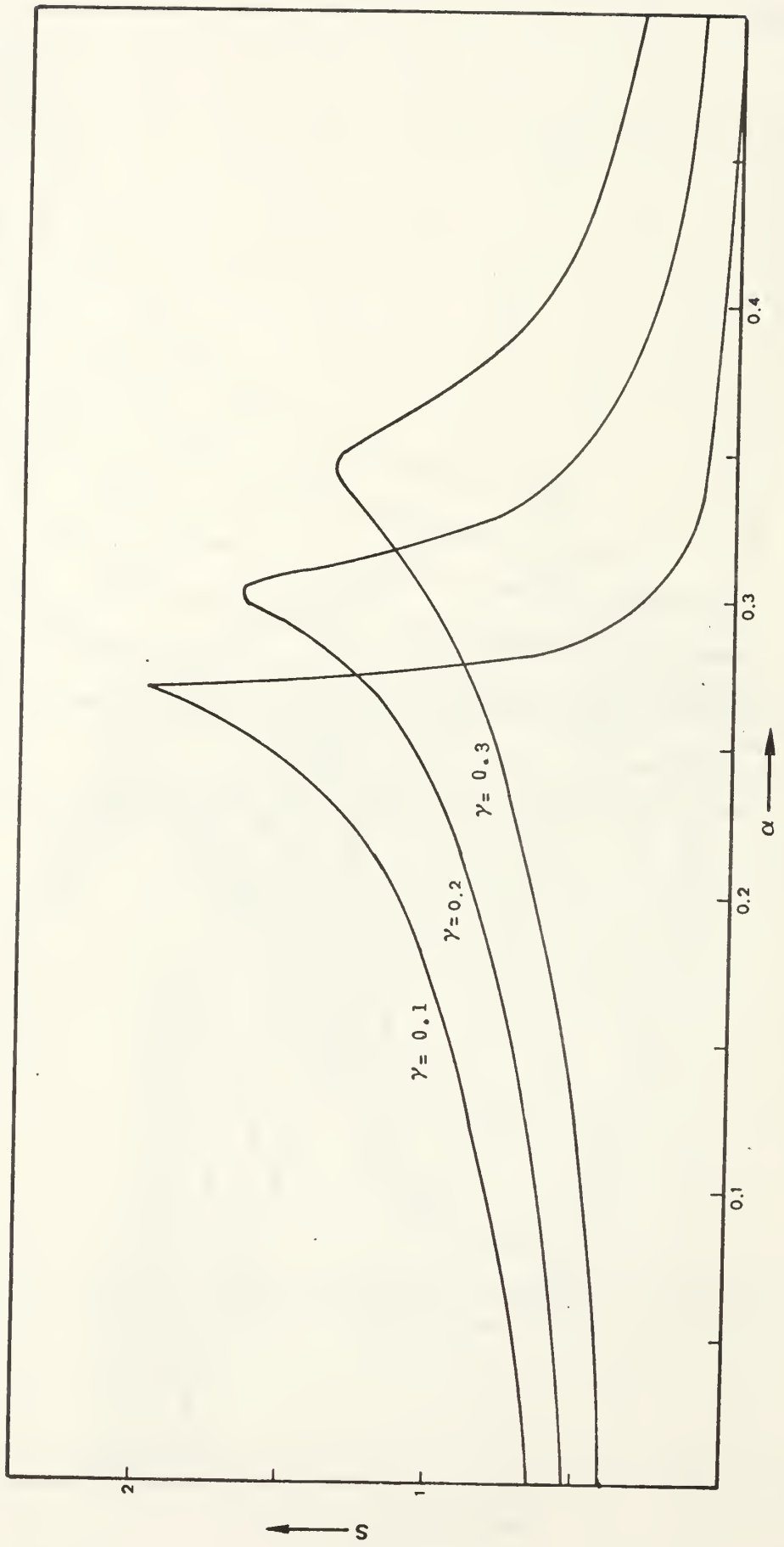
γ= 0.1
γ=0.2
γ= 0.3
0.1
0.2
0.3
0.4
α
1
2
S

DISTRIBUTION LIST

		No. Copies
1.	Defense Documentation Center Cameron Station Alexandria, Virginia 22314	12
2.	Library, Code 0212 Naval Postgraduate School Monterey, California 93940	2
3.	Dr. A. L. Schoenstadt, Code 53Zh Department of Mathematics Naval Postgraduate School Monterey, CA 93940	10
4.	Dr. R. T. Williams, Code 51Wu Department of Meteorology Naval Postgraduate School Monterey, California 93940	15
5.	Commanding Officer Naval Weather Service Command Headquarters 3101 Building 200 Washington Navy Yard Washington, D. C. 20374	1
6.	Officer in Charge Environmental Prediction Research Facility Naval Postgraduate School Monterey, California 93940	10
7.	Dean of Research Naval Postgraduate School Monterey, California 93940	2
8.	Commanding Officer Fleet Numerical Weather Central Naval Postgraduate School Monterey, California 93940	10
9.	Naval Oceanographic Office Library (Code 3330) Washington, D. C. 20373	1
10.	AFCRL - Research Library L. G. Hanscom Field ATTN: Nancy Davis/Stop 29 Bedford, Massachusetts 01730	1

11. Commander, Air Weather Service — 1
Military Airlift Command
United States Air Force
Scott Air Force Base, Illinois 62226

12. Dr. R. L. Alberty — 1
National Severe Storms Laboratory
University of Oklahoma
Norman, Oklahoma 73069

13. Dr. R. Alexander — 1
The RAND Corporation
1700 Main Street
Santa Monica, California 90406

14. Dr. A. Arakawa — 1
Department of Meteorology
University of California
Los Angeles, California 90024

15. Dr. D. Archer — 1
Mathematics Department
University of North Carolina
UNCC Station
Charlotte, North Carolina 28223

16. Atmospheric Sciences Library — 1
National Oceanic and Atmospheric Administration
Silver Spring, Maryland 20910

17. Mr. E. Barker — 1
Environmental Prediction Research Facility
Naval Postgraduate School
Monterey, California 93940

18. Dr. F. P. Bretherton — 1
National Center for Atmospheric Research
P. O. Box 3000
Boulder, Colorado 80303

19. Dr. John Brown — 1
National Meteorological Center/NOAA
World Weather Building
Washington, D. C. 20233

20. Dr. C. P. Chang, Code 51Cj — 1
Department of Meteorology
Naval Postgraduate School
Monterey, California 93940

21. Professor J. G. Charney 1
54-1424
Massachusetts Institute of Technology
Cambridge, Massachusetts 02139

22. Dr. C. Comstock, Code 53Cs 1
Department of Mathematics
Naval Postgraduate School
Monterey, California 93940

23. Dr. D. Dietrick 1
Code 7750
Naval Research Laboratory
Washington, D. C. 20390

24. Dr. R. L. Elsberry, Code 51Es 1
Department of Meteorology
Naval Postgraduate School
Monterey, California 93940

25. Dr. Frank D. Faulkner, Code 53Fa 1
Mathematics Department
Naval Postgraduate School
Monterey, California 93940

26. Dr. Richard Franke, Code 53Fe 1
Department of Mathematics
Naval Postgraduate School
Monterey, California 93940

27. Dr. J. A. Galt 1
NOAA - Pac. Mar. Envir. Lab.
University of Washington WB-10
Seattle, Washington 98105

28. Dr. W. L. Gates 1
The RAND Corporation
1700 Main Street
Santa Monica, California 90406

29. Dr. G. J. Haltiner, Code 51Ha 1
Chairman, Department of Meteorology
Naval Postgraduate School
Monterey, California 93940

30. Dr. R. L. Haney, Code 51Hy 1
Department of Meteorology
Naval Postgraduate School
Monterey, California 93940

31. Dr. J. Holton — 1
Department of Atmospheric Sciences
University of Washington
Seattle, Washington 98105

32. Dr. B. J. Hoskins — 1
Department of Geophysics
University of Reading
Reading
United Kingdom

33. Dr. D. Houghton — 1
Department of Meteorology
University of Wisconsin
Madison, Wisconsin 53706

34. Dr. Joseph Huang — 1
Great Lake Environmental Res. Lab.
NOAA
2300 Washtenaw Avenue
Ann Arbor, Michigan 48104

35. Dr. S. K. Kao — 1
Department of Meteorology
University of Utah
Salt Lake City, Utah 84112

36. Dr. A Kasahara — 1
National Center for Atmospheric Research
P. O. Box 3000
Boulder, Colorado 80303

37. Dr. C. E. Leith — 1
National Center for Atmospheric Research
P. O. Box 3000
Boulder, Colorado 80303

38. Dr. J. M. Lewis — 1
Laboratory for Atmospheric Research
University of Illinois
Urbana, Illinois 61801

39. Dr. E. N. Lorenz — 1
Department of Meteorology
Massachusetts Institute of Technology
Cambridge, Massachusetts 02139

40. Dr. R. Madala — 1
Code 7750
Naval Research Laboratory
Washington, D. C. 20390

41. Dr. J. D. Mahlman — 1
Geophysical Fluid Dynamics Laboratory
Princeton University
Princeton, New Jersey 08540

42. Dr. G. Morris, Code 53Mj — 1
Department of Mathematics
Naval Postgraduate School
Monterey, California 93940

43. Meteorology Library (Code 51) — 1
Naval Postgraduate School
Monterey, California 93940

44. LT. W. F. Mihok — 1
Fleet Numerical Weather Central
Naval Postgraduate School
Monterey, California 93940

45. Dr. S. Mudrick — 1
AFCRL (YD)
L. G. Hanscom Field
Bedford, Massachusetts 01730

46. National Center for Atmospheric Research — 1
Box 1470
Boulder, Colorado 80302

47. Director, Naval Research Laboratory — 1
ATTN: Technical Services Information Center
Washington, D. C. 20390

48. Dr. E. C. Nickerson — 1
NOAA
Atmospheric Physics and Chemistry Laboratory
Boulder, Colorado 80302

49. Department of Oceanography, Code 58 — 1
Naval Postgraduate School
Monterey, California 93940

50. Office of Naval Research — 1
Department of the Navy
Washington, D. C. 20360

51. Dr. T. Ogura — 1
Laboratory for Atmospheric Research
University of Illinois
Urbana, Illinois 61801

52. Professor K. Ooyama 1
National Center for Atmospheric Research
P. O. Box 3000
Boulder, Colorado 80303

53. Professor N. A. Phillips 1
National Meteorologican Center/NOAA
World Weather Building
Washington, D. C. 20233

54. Dr. S. Piacsek 1
Code 7750
Naval Research Laboratory
Washington, D. C. 20390

55. Dr. T. Rosmond 1
Environmental Prediction Research Facility
Naval Postgraduate School
Monterey, California 93901

56. Dr. F. Sanders 1
Department of Meteorology
Massachusetts Institute of Technology
Cambridge, Massachusetts 02139

57. Dr. Y. Sasaki
Environmental Prediction Research Facility 1
Naval Postgraduate School
Monterey, California 93940

58. Dr. Fred Shuman, Director 1
National Meteorological Center
World Weather Building
Washington, D. C. 20233

59. Dr. Joanne Simpson 1
Department of Environmental Sciences
2015 Ivy Road
Charlottesville, Virginia 22903

60. Dr. R. Somerville 1
NCAR
P. O. Box 3000
Boulder, Colorado 80303

61. Dr. D. Williamson 1
National Center for Atmospheric Research
P. O. Box 3000
Boulder, Colorado 80303

62. Dr. F. J. Winninghoff — 1
1085 Steeles Avenue, #503
Willowdale (Toronto)
Ontario M2R2T1 Canada

63. Dr. M. G. Wurtele — 1
Department of Meteorology
University of California
Los Angeles, California 90024

64. Dr. J. Young — 1
Department of Meteorology
University of Wisconsin
Madison, Wisconsin 53706

65. Dr. L. D. Kovach, Code 53Kv — 1
Chairman, Department of Mathematics
Naval Postgraduate School
Monterey, California 93940

[redacted]

NPS